

Anh Le

**MODELLING WATER-ALCOHOL MIXTURE ADSORPTION ON
ZEOLITES**

Thesis

CENTRIA UNIVERSITY OF APPLIED SCIENCES

Environmental Chemistry and Technology

June 2020

ABSTRACT

Centria University of Applied Sciences	Date June 2020	Author Anh Le
Degree programme Environmental Chemistry and Technology		
Name of thesis MODELLING WATER- ALCOHOL MIXTURE ADSORPTION ON ZEOLITES		
Instructor DSc (Tech.) Jani Kangas	Pages 38+2	
Supervisor Laura Rahikka- Nina Hynynen		
<p>The aim of this thesis was to analyze and predict the adsorption of water-ethanol mixtures on four types of zeolitic materials: CHA, DDR, MFI, and FAU. The adsorption behavior was evaluated based on the extent of ethanol and water loading as function of total fugacity and partial fugacity. The isotherm illustrated by loading- partial fugacity is unary isotherm, then the saturation loading defined from these figures. The binary isotherm is shown by loading- total fugacity figures. Increasing total fugacity, the system adsorbs preferentially water molecules. However, FAU is exceptional because it is a Hydrophilic membrane.</p> <p>IAST and RAST can be used to predict water-ethanol adsorption on different adsorbents. IAST stands for ideal adsorption solution theory. This method assumes that the adsorption behaves ideally. RAST means Real Adsorption Solution Theory, which is derived from IAST method. It differs from IAST method because of introducing of activity coefficient in calculation. The deviation of RAST from IAST is compared to define the effect of activity coefficient on adsorption behaviors. In this study, the IAST and RAST were applied as mixture adsorption models. The models had been implemented in the MATLAB environment.</p> <p>Among these hydrophobic zeolites: CHA, MFI, DDR; selectivity result shows that CHA is the most efficient zeolite in separation of water and ethanol mixture at low fugacity, followed by MFI, then DDR. FAU zeolite is suitable for dehydration of ethanol.</p>		

Key words

Adsorption isotherm, Zeolite, IAST, RAST

CONCEPT DEFINITIONS

P_i^0 : pressure for sorption of every component i

q_i^0 : pure component isotherm $\left(\frac{\text{mol}}{\text{kg}}\right)$

A Surface area per kg of framework (m^2 per kg of the framework of crystallized material)

b: Adsorption equilibrium parameter (1/Pa)

C: Wilson constant used in Eq. (14)

d_p : pore diameter of membrane, Å

E: Energy (J/mol)

f_i : Partial fugacity, Pa

f : Total fugacity, Pa

p_i : partial pressure for component i

p : total system pressure, Pa

q_i : Molar loading of component i in the adsorbed phase (mol/kg of framework)

$q_{i, \text{sat}}$: Molar loading of component i at saturation (mol/kg of framework)

R : Gas constant, J/(mol·K)

S : selectivity

S_g : surface area of adsorbent (m^2/g)

T : absolute temperature, K

x_i : Mole fraction of component i in adsorbed phase, dimensionless

y_i : Mole fraction of component i in bulk fluid mixture, dimensionless

K: equilibrium constant

Greek symbol

π : Spreading pressure (same unit as surface tension, e.g. Nm^{-1})

μ : Molar chemical potential (J/mol)

ε : porosity of pore membrane, dimensionless

ρ : density of adsorbent (g/cm^3)

γ : activity coefficient, dimensionless

F : thermodynamic factors, dimensionless

A : Wilson parameter, dimensionless

Subscript

n : number of species in mixture, dimensionless

i : component i in mixture

p: pore or particle

g: gas

Abbreviation

FAU: Faujasite (Zeolite framework type)

MFI: Mordenite framework inverted (Zeolite framework type)

CHA: Chabazite (Zeolite framework type)

DDR: Deca- Dodecasil 3 Rhombohedral (Zeolite framework type)

IAST: Ideal adsorbed solution theory

RAST: Real adsorbed solution theory

sat: saturated

exp: exponential function

BET: Brunauer-Emmet-Teller

TABLE OF CONTENTS

ABSTRACT

CONCEPT DEFINITIONS

1 INTRODUCTION.....	1
2 THEORY	3
2.1 Adsorbents	3
2.2 Zeolites	4
2.3 Adsorption	5
3 ADSORPTION MODELS.....	8
3.1 Pure component adsorption isotherms.....	9
3.1.1 Henry's law.....	9
3.1.2 Langmuir isotherm	9
3.1.3 Freundlich isotherm.....	10
3.2 Multicomponent adsorption models	12
3.2.1 IAST	12
3.2.2 Activity coefficients and RAST	14
3.3 Selectivity equilibrium	14
4 HYDROGEN BONDING AND MOLECULAR CLUSTERING	15
5 MATERIAL AND METHODS	17
5.1 Material.....	17
5.2 Method	20
5.2.1 Modelling water ethanol mixture loading on a zeolite as a function of partial fugacity	20
5.2.2 Modelling water ethanol mixture loading on a zeolite as a function of total fugacity	20
5.2.3 Comparison of ethanol loading in different membranes.....	20
6 RESULTS	22
6.1 Loading mass as function of partial fugacity.....	22
6.1.1 FAU	22
6.1.2 MFI.....	23
6.1.3 DDR.....	24
6.1.4 CHA.....	25
6.2 Loading mass as function of total fugacity	26
6.2.1 MFI.....	27
6.2.2 FAU	27
6.2.3 DDR.....	29
6.2.4 CHA.....	30
6.3 Comparison of ethanol loadings on different zeolites.....	31
6.4 Ethanol/Water adsorption selectivity	32
7 DISCUSSION	34

8 CONCLUSION	35
REFERENCES.....	37

APPENDICES

FIGURES

FIGURE 1. Adsorption concept of two components	6
FIGURE 2. Type of isotherm	8
FIGURE 3. a) Molecule distribution, no clustering, b) Molecule distribution, clustering	16
FIGURE 4. Adsorbed loadings of water and ethanol on a FAU zeolite as predicted by IAST and RAST.	23
FIGURE 5. Adsorbed loadings of water and ethanol on MFI-zeolite at different fugacities with IAST and RAST.....	24
FIGURE 6. Adsorbed loadings of water and ethanol on DDR-zeolite at different fugacities with IAST and RAST.....	25
FIGURE 7. Adsorbed loadings of water and ethanol on CHA-zeolite at different fugacities with IAST.	26
FIGURE 8. Adsorbed loadings of water and ethanol on MFI-zeolite at different total fugacities with RAST..	27
FIGURE 9. Adsorbed loadings of water and ethanol on FAU-zeolite at different total fugacities with RAST..	28
FIGURE 10. Adsorbed loadings of water and ethanol on DDR-zeolite at different total fugacities with RAST.	29
FIGURE 11. Adsorbed loadings of water and ethanol on CHA-zeolite at different total fugacities with IAST.....	30
FIGURE 12. Ethanol loading (mol/kg) on different type of membrane at 300K, $f_1=f_2$	31
FIGURE 13. Selectivity on different type of membrane, Ethanol/Water	32

TABLES

TABLE 1. Representative Properties of Commercial Adsorbent.	4
TABLE 2. Some important zeolite adsorbents and their application	5
TABLE 3. Other isotherms	11
TABLE 4. Zeolite pore diameter and type.....	17
TABLE 5. Dual-site Langmuir-Freundlich parameters for adsorption of water and ethanol at 300 K in all-silica FAU zeolite	18
TABLE 6. Dual-site Langmuir-Freundlich parameters for pure component water and ethanol at 300 K in all-silica DDR zeolite.....	18
TABLE 7. Dual-site Langmuir-Freundlich parameters for adsorption of water, methanol, and ethanol at 300 K in all-silica MFI zeolite	19
TABLE 8. Dual-site Langmuir-Freundlich parameters for pure component water, and 1-alcohols in CHA at 300K	19
TABLE 9. Wilson non-ideality parameters for binary water/ethanol mixture adsorption	19

1 INTRODUCTION

The change from fossil fuels to biofuels is of high demand because of the drainage of crude oil. Currently, the main commercially used biofuels worldwide are bioethanol, biodiesel, and biogas. Ethanol is produced commercially by fermentation of starch or sugar-based crops. Ethanol produced by fermentation has at maximum only 15 wt.% of ethanol rest being water (Mohanty & Purkait 2011, 68). Dehydrated ethanol is used as a blend of gasoline; however, the water concentration in the mixture must be lower than 2000 ppm (Zou & Zhu 2019). Besides distillation and molecular sieve drying, ethanol can also be separated from an ethanol/water mixture by pervaporation process.

The dehydration of ethanol using membranes can be conducted by applying hydrophilic or hydrophobic membranes. A hydrophilic membrane favors absorbing water and rejecting an organic molecule, e.g. ethanol. Hydrophobic membrane prefers to adsorb organic molecule; thus, water molecule is retained on the feed side of the membrane. Pervaporation works based on membrane technology; it be a cost-effective compared to other methods. A combination of distillation and pervaporation is called as “a hybrid process” (Slater 1991). The operating principle of pervaporation is a combination of diffusion and adsorption behavior. Components are first adsorbed on the zeolitic film, then they diffuse with different rates through the membrane pores and evaporate on the other side. For an economic separation process, the adsorbent should possess these properties: it should have significantly high selectivity between the adsorbates, capacity of the wanted compound, and durability in the conditions. (Ruthven 1984.)

This thesis focuses on the investigation of the adsorption behaviors of various type zeolitic adsorbents; they are namely CHA, FAU, DDR, MFI. Generally, the determination of the most suitable adsorbent is the first step for efficient separation process design. In the separation process, thermodynamic potential is assumed to affect the separation selectivity and efficiency of the process. Thus, the adsorption behavior is evaluated accordingly to thermodynamics. Molecular size of a component is also a factor affecting the separation process. A comprehensive evaluation of separation of a gas mixture on a zeolite membrane must include three factors: sizes of the gas molecules, thermodynamic selectivity, and kinetic selectivity. Thermodynamic selectivity explains that when more than one component enters the pore, the entropy of the system favors one component in adsorbing over the others. Kinetic selectivity shows the ability of one component entering the pores faster than the others. (Kangas 2014, 29.)

The correlation, analysis, and prediction of adsorption equilibria of gaseous mixtures on microporous membrane are approached through this thesis. There are many calculation methodologies for predicting adsorption of mixture/ pure component, such as: IAST, RAST, PRAST, VST and MPTA. VST and MPTA have been investigated less than the other methods in the literature. The limit of MPTA is that it has difficulties in calculation of multicomponent distributions released by the adsorbent. IAST and RAST are mainly applied and discussed for determining equilibria of water/ ethanol mixture. (Kangas 2014, 33-41.)

2 THEORY

Separation Technologies include many processes such as distillation, adsorption, liquid- liquid extraction and ion exchange. The separation process by phase addition or creation are adsorption and stripping of dilute mixture, Distillation of binary mixture and Batch distillation. Membrane separation, Adsorption, Ion exchange Chromatography and Electrophoresis belong to separation process by barriers and solid agent. Leaching and washing, Crystallization, Desublimation, Evaporation, and drying of solid are categorized as separation process involving a solid phase. Adsorption is an alternative method for distillation, because of its economic benefit. The adsorption mechanism can be chemical adsorption or physical adsorption, or both. (Seader et al 2010; Ruthven 1984.)

2.1 Adsorbents

There are many types of adsorbents such as: silica-gel, activated alumina, activated carbon, carbon molecular sieve, and zeolite. Table 1 shows the characteristic parameters of some common adsorbents. Adsorbent can be hydrophilic or hydrophobic material. A hydrophilic adsorbent prefers to adsorb water while a hydrophobic, or organophilic, material means that the material rejects water adsorption. The pore diameter of an adsorbent varies from 2 Å to 150 Å. According to the International Union of Pure and Applied Chemistry 1982, there are three types of adsorbents classified according to their pore sizes: Microporous adsorbent has pore size smaller than 20 Å, Mesoporous adsorbent's pore size varies from 20 Å to 500 Å and Macroporous adsorbent's pore size is larger than 500 Å. (Sader et al 2010, 571-573.) Table 1 shows common membranes and their nature.

TABLE 1. Representative Properties of Commercial Adsorbent (Sader et al. 2010, 572).

Adsorbent	Nature	Pore Diameter d_p (Å)	Particle Porosity, ϵ_p	Particle Density ρ_p (g/cm ³)	Den- Surface Area S_g (m ² /g)	Capacity for H ₂ O Vapor at 25°C and 4.6 mmHg. (wt% dry basis)
Activated alumina	Hydrophilic, amorphous	10-75	0.5	1.25	320	7
Silica gel:	Hydrophilic/hydrophobic,					
Small pore	amorphous	22-26	0.47	1.09	750-850	11
Large pore		100-150	0.71	0.62	300-350	–
Activated carbon:	Hydrophobic, amorphous					
Small pore		10-25	0.4-0.6	0.5-0.9	400-1200	1
Large pore		>30	–	0.6-0.8	200-600	–
Molecular-sieve carbon	Hydrophobic	2-10	–	0.98	400	–
Molecular sieve zeolites	Polar-philic, Hydro-crystalline	3-10	0.2-0.5	1.4	600-700	20-25
Polymeric adsorbents	–	40-25	0.4-0.55	–	80-700	–

2.2 Zeolites

Zeolites, and other molecular sieves, are separation media used in the adsorption of different compounds. Zeolites originate from natural or synthetic aluminosilicates, which have fine porous structure. Adsorption on molecular sieves is applied among others for the separation of oxygen from nitrogen, in the production of pure hydrogen from synthesis gas, and categorization of specific paraffin from branched paraffin and aromatics. (McCabe et al. 2005.)

A zeolite is structurally crystalline assemblage of SiO₄ and AlO₄ tetrahedra, PO₄ in some case, joint together by an oxygen bridge. Different kinds of units are formed by tetrahedra, such as 6-rings, 8-rings, or 12-rings (Smit et al. 2014). Zeolites are categorized into Zeolite A, Zeolite X and Y, Mordenite and Pentasil zeolite. Within the zeolite there exists space in crystal lattice configuration for guest molecule

to penetrate through the lattice (Ruthven, 1984). Table 2 shows some important zeolites and their applications.

TABLE 2. Some important zeolite adsorbents and their applications (Ruthven 1984, 25).

Framework	Cationic form	Formula of Typical unit cell	Window	Effective channel diameter(Å)	Application
A	Na	$\text{Na}_{12}[(\text{AlO}_2)_{12}(\text{SiO}_2)_{12}]$	8- ring (Obstructed)	3.8	CO_2 removal from natural gas
	Ca	$\text{Ca}_5\text{Na}_2[(\text{AlO}_2)_{12}(\text{SiO}_2)_{12}]$	8- ring (free)	4.4	Linear paraffin separation. Air separation
	K	$\text{K}_{12}[(\text{AlO}_2)_{12}(\text{SiO}_2)_{12}]$	8- rings (Obstructed)	2.9	Drying of crack gas containing CH_4
X	Na	$\text{Na}_{86}[(\text{AlO}_2)_{86}(\text{SiO}_2)_{106}]$	12- ring	8.4	Pressure swing H_2 purification
	Ca	$\text{Ca}_{40}\text{Na}_6[(\text{AlO}_2)_{86}(\text{SiO}_2)_{106}]$	12- ring	8	Removal of mercaptans from natural gas
	Sr, Ba(=KBaX)	$\text{Sr}_{21}\text{Ba}_{22}[(\text{AlO}_2)_{86}(\text{SiO}_2)_{106}]$	12- ring	8	Xylene separation
Y	Na	$\text{Na}_{56}[(\text{AlO}_2)_{56}(\text{SiO}_2)_{136}]$	12- ring	8	Xylene separation
	K	$\text{K}_{56}[(\text{AlO}_2)_{56}(\text{SiO}_2)_{136}]$	12- ring	8	Xylene separation
Mordenite	Ag	$\text{Ag}_8[(\text{AlO}_2)_8(\text{SiO}_2)_{40}]$	12- ring	7	I and Kr removal from nuclear off - gases
	H	$\text{H}_8[(\text{AlO}_2)_8(\text{SiO}_2)_{40}]$	12- ring		
Silicalite	-	$(\text{SiO}_2)_{96}$	10- ring	6.0	Removal of organics from water
ZSM-5		$\text{Na}_3[(\text{AlO}_2)_3(\text{SiO}_2)_{93}]$	10- ring	6	Xylene separation

2.3 Adsorption

Adsorption is a separation process in which a molecule from fluid bulk is attracted towards the surface of solid adsorbent due to physical forces or chemical bonding. In adsorption, the adsorbed solute is an adsorbate, the solid material adsorbing the adsorbate is an adsorbent. Adsorbents are normally porous materials; adsorption occurs on the surface of a pore. The adsorption efficiency depends on the solid-fluid equilibria and mass transfer rate. Because of differences in physical and chemical characteristics,

such as polarity, molecular weight and shape, some molecules diffuse through the pore, while the others are stuck on the solid surface. (Mc Cabe et al. 2005.)

Adsorption can occur both from gas/vapor phase or liquid phase. Vapor phase adsorption is widely used to recover organic solvents in paints, printing ink industry and to remove volatile compounds from effluent vapor streams. Liquid phase adsorption is applied in liquid waste treatment to remove organic components. It is utilized in the removal of impurities from sugar solution and vegetable oil, and water from organic liquid. It is an alternative separation method when distillation and crystallization are not applicable. Through the past decade, the adsorption application has been expanding, which includes separation of water/alcohol mixture using zeolite membrane. (Mc Cabe et al. 2005) Figure 1 shows the adsorption concept when two components are adsorbing on a porous adsorbent.

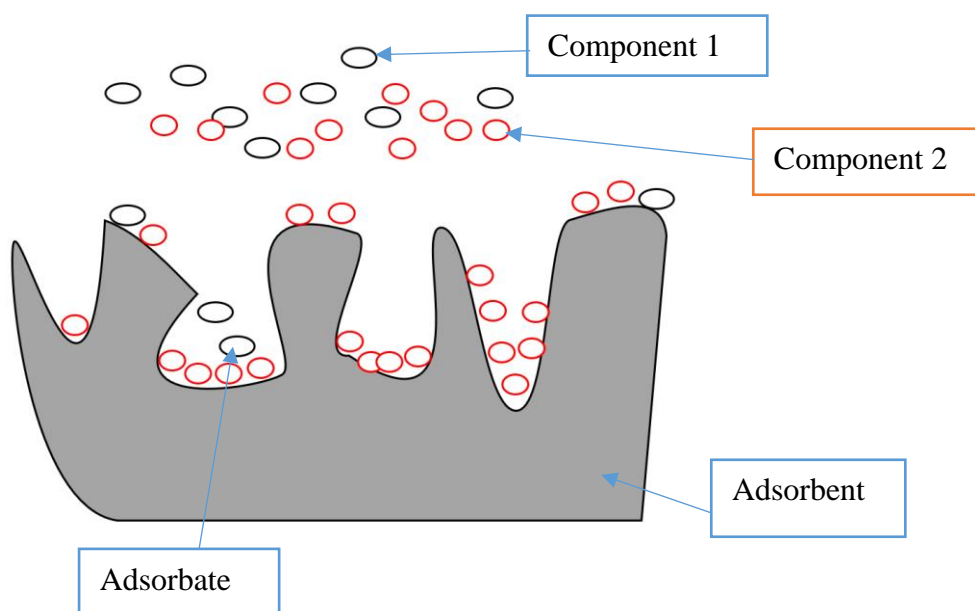


FIGURE 1. Adsorption concept of two components. (Keller et al. 2005, 19)

As can be seen in Figure 1, the adsorption system has two components, which are black and red round-shape. Component 1 is larger than component 2. When the components deposit on the surface of the adsorbent, they are adsorbate including both component 1 and component 2. Adsorption is the stage when molecule binds on the adsorbent surface. Then, part of molecules diffuses through the membrane pore.

Adsorption is classified mainly into physisorption and chemisorption based on the forces between fluid molecules and solid molecules; van der Waals forces means physical adsorption, and activated forces means chemisorption. (Mc Cabe et al. 2005.) However, the adsorption phenomena occurring during separation is complex, so combination of the physical and chemical adsorption phenomena may also occur.

When physisorption occurs (normally at low temperatures), the adsorbates form a monomolecular layer before multilayers due to interaction between molecules; in case the pore's size is similar to molecule's size, then capillary condensations occurring causes pores filled with adsorbate. Even though polarization may take place, there is no transfer electron. Chemisorption occurs at high temperature when chemical bonds between adsorbent and adsorbate forms. It is slow and irreversible, the adsorbate forms only monolayer. (Ruthven 1984, 29.) Evaporation is a process when component changes from liquid phase into vapor phase (Encyclopædia Britannica, evaporation 2020). The adsorptive separation processes mostly based on the physical adsorption principle.

3 ADSORPTION MODELS

Adsorption isotherms describe the relationship between the concentration of the compound in the fluid phase and the distribution of the same compound on the adsorbent surface at the given temperature. The concentration of adsorbate on the solid is generally illustrated by mass of adsorbed per unit of initial mass adsorbate. (Keller & Staudt 2005; Seader et al. 2010.) There are six types of isotherms shown in Figure 2.

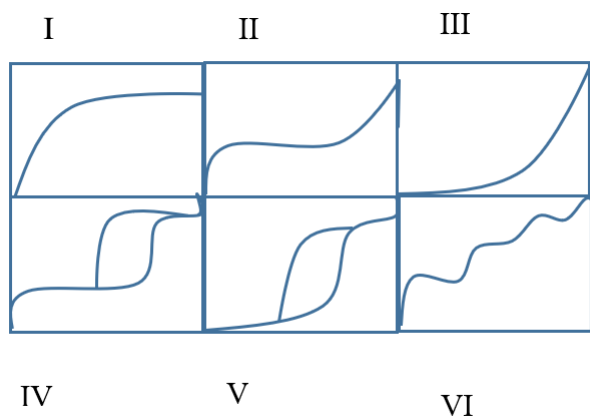


FIGURE 2. Type of isotherm (IUPAC, 1985)

Type I is the common isotherm for microporous adsorbent, and it shows the maximum amount adsorbed corresponding to complete filling of microporous, but no multilayer is formed. In this case, the pore size of the adsorbent is not much larger than the molecular diameter of the sorbate molecules. Type I can be explained by Langmuir isotherm. The mass loading adsorbed and maintained even at high pressure is known as asymptotic value. When the adsorbent has various sized pores, adsorption occurs following type II and type III isotherms. The adsorption in mesoporous adsorbent normally follows type II isotherm. The loading increases until it forms a monolayer at low pressure, then at high pressure near saturation point, multilayer is formed, and capillary condensation is formed, but no hysteresis occurs. Type III shows that the interaction between adsorbate-sorbent is smaller than adsorbate-adsorbate. (Keller & Staudt 2005; Seader et al. 2010.)

From type IV, it can be predicted that there is a formation of two layers either on the plane surface or on the wall of a pore, which is much wider than the molecular diameter of sorbate. Type V suggests that intermolecular interaction affects the adsorption process. Type IV and type V illustrate the hysteresis behavior between adsorption and desorption branch. In all case, the adsorption does not occur after saturated pressure. The flat intermediate area in type II and type IV is because of monolayer formation.

Type VI describes the stepwise formation of multilayer adsorption. (Keller & Staudt 2005; Seader et al. 2010.)

3.1 Pure component adsorption isotherms

The concern of equilibria is necessary for predicting the adsorption behavior. The adsorption behavior of single component is illustrated by pure component adsorption isotherms. Some common isotherms are Langmuir Adsorption isotherm, Freundlich isotherm, Henry's law... These isotherms express the adsorption equilibria based on various assumptions.

3.1.1 Henry's law

Henry's law is the simplest of the pure component adsorption isotherms. The Henry law states that the relationship between fluid phase and adsorbed phases concentration will be linear. According to the Henry's law, the loading of a pure component can be described with the relation:

$$q = K_{H,i}P, \quad (1)$$

where q is loading (mol/kg framework),
 $K_{H,i}$ is Henry constant of component i (mol kg⁻¹ Pa⁻¹), and
 P is pressure (Pa).

Henry's law is only applicable for the linear region of isotherm equilibrium measurement because at high pressure, the relationship between loading and pressure is invalid due to the adsorbate interactions. (Ruthven 1984; Malara et al. 1992.)

3.1.2 Langmuir isotherm

Langmuir isotherm can be described with a type I isotherm. It shows good results when used to describe microporous adsorption. Because of tiny pore size, only a few molecules are adsorbed within a pore and permeate before saturation. Thus, there is no chance for significant interaction between them. The Langmuir isotherm can be used to describe adsorption on zeolite. Langmuir isotherm is only applied when the process meet these assumptions: the adsorbates are on an unchanged number of sites, each side can

adsorb only one component, the energy is equal in every site, and it is monolayer adsorption only. Furthermore, there is no interaction between adsorbed molecules. (Malara et al. 1992.) The relationship between loading and pressure according to the Langmuir isotherm is shown in Eq. (2):

$$q_i = \frac{q_i^{sat} b_i P}{1 + b_i P}, \quad (2)$$

where b_i is adsorption equilibrium constant, (Pa^{-1}),
 q_i is loading of component i , (mol/kg) and
 q_i^{sat} is maximum loading of component i , (mol/kg).

As can be seen in Eq. (2), at high pressure the loading of a compound approaches its saturation loading, i.e. $q_i \rightarrow q_i^{sat}$. Langmuir adsorption isotherm shows non-linearity as a function of pressure and predicts an asymptotic limit for q , which cannot be done based on Freundlich equation, which is introduced in the next chapter. When the system approaches maximum loading point (q_i^{sat}), zeolite is completely covered by adsorbate; thus, Langmuir isotherm is commonly applied for monolayer adsorption. (Keller & Staudt 2005; Seader et al. 2010.)

3.1.3 Freundlich isotherm

Freundlich isotherm is an empirical isotherm, and limited application in a range of adsorption equilibrium data. It does not predict the asymptotic limit for q at high pressure. Furthermore, it also does not obey Henry law at low pressure. The adsorption isotherm can be described with a Freundlich isotherm, which is shown in Eq. (3):

$$q = K_{F,i} P^{\frac{1}{n}}, \quad (3)$$

where $K_{F,i}$ is Freundlich constant of component i , and
 n is Freundlich constant.

There are some other isotherms such as: Sips, Tóth, BET and Dubinin- Raduschkevich. The forms of the isotherms are shown in Table 3. The Dual Langmuir-Freundlich isotherm shown in Table 3 is formed from the mass balance between condensation of generic layer and the evaporation from the adjacent

layer. It is applicable if the system satisfies the assumption which are: Every first layer molecule forms an adsorption site for a second layer molecule and so on. Besides, the interactions between the various layers of molecules are neglected. Furthermore, the first layer adsorption heat is different from that of the successive layers, which are equal and equal to the liquefaction heat of the liquid bulk surface.

TABLE 3. Other isotherms (Leppäjärvi 2015, 36)

Isotherm	Mathematical form
Sips	$q_i = \frac{q_i^{sat} (b_i P)^{1/n}}{1 + (b_i P)^{1/n}}$
Tóth	$q_i = \frac{q_i^{sat} b_i P}{[1 + (b_i P)^n]^{1/n}}$
BET	$q_i = \frac{q_i^{sat} c_i \left(\frac{P}{P_i^{sat}}\right)}{\left(1 - \frac{P}{P_i^{sat}}\right) \left(1 - \frac{P}{P_i^{sat}} + c_i \frac{P}{P_i^{sat}}\right)}$
Dubinín- Raduschévich	$q_i = q_i^{sat} \exp \left\{ - \left[\frac{RT}{E} \ln \left(\frac{P_i^{sat}}{P} \right) \right]^2 \right\}$
Dual Langmuir-Freundlich	$q^0(f) = q_{A,sat} \frac{b_A f^{vA}}{1 + b_A f^{vA}} + q_{B,sat} \frac{b_B f^{vB}}{1 + b_B f^{vB}}$

3.2 Multicomponent adsorption models

The adsorption models of multicomponent mixture are calculated by IAST or RAST methodologies. IAST stands for Ideal Adsorbed Solution Theory, which is applied for ideal mixture only. RAST means Real Adsorbed Solution Theory, it is developed from IAST method by proposing activity coefficient into calculation.

3.2.1 IAST

The ideal adsorbed solution theory (IAST) was established by Mayer and Prausnitz in 1965. It aims to predict the adsorption behavior of multicomponent mixture based on pure component isotherm, also known as unary isotherm. The key assumption for this method is both the bulk phase and adsorbed phase behave ideally. By comparing data calculation by IAST method with data collected from the CMBC (Configurational Bias Monte Carlo) simulation, it is concluded that there are two cases when the IAST does not provide an adequate accuracy data, which are: Molecular clustering formed by strong hydrogen bonding between the adsorbates. Moreover, when guest molecule is prioritized in siting and location, it causes the inhomogeneous, isolated distribution of adsorbate within the pore network. (Krishna 2018) Because of the existence of guest molecule in adsorbed phase, Gibbs adsorption is shown in a different form. Gibbs Adsorption equation:

$$Ad\pi = \sum_{i=1}^n q_i d\mu_i, \quad (4)$$

where μ_i is the chemical potential of compound i .
 A is the surface area per mass unit of framework (m^2/kg of framework), and
 π is the spreading pressure, same unit as surface tension, (N/m).

It is noteworthy that the chemical potentials (μ_i) of any component in adsorbed phase and bulk phase are the same. The differential of chemical potential (μ_i) is equal to

$$d\mu_i = RT d \ln f_i. \quad (5)$$

The equation of partial fugacity of component i in the bulk phase (f_i) according to IAST is:

$$f_i = P_i^0 x_i, \quad i=1;2;3\dots n \quad (6)$$

the correlation between mole fraction (x_i) and loading is given with:

$$x_i = \frac{q_i}{q_1+q_2+\dots+q_n}. \quad (7)$$

The pressure for sorption of every component i (P_i^0) provide the same spreading pressure π , for each pure component, then the adsorption potential is:

$$\frac{\pi A}{RT} = \int_0^{P_1^0} \frac{q_1^0(f)}{f} df = \int_0^{P_2^0} \frac{q_2^0(f)}{f} df \dots \quad (8)$$

The adsorption potential has the same unit with loading either mol kg⁻¹ or molecules per unit cell. The pure compound isotherm can be any of the models presented in the previous chapters. When Dual Langmuir-Freundlich isotherm is applied, the integral of Eq. (8) is:

$$\int_{f=0}^{P_i^0} \frac{q^0(f)}{f} df = \frac{q_{A,sat}}{v_A} \ln (1 + b_A (P_i^0)^{v_A}) + \frac{q_{B,sat}}{v_B} \ln (1 + b_B (P_i^0)^{v_B}) . \quad (9)$$

$$\int_{f=0}^{P_i^0} \frac{q^0(f)}{f} df = \frac{q_{A,sat}}{v_A} \ln (1 + b_A (\frac{f_i}{x_i})^{v_A}) + \frac{q_{B,sat}}{v_B} \ln (1 + b_B (\frac{f_i}{x_i})^{v_B}). \quad (10)$$

The variable in Eqs. (10)-(11) must satisfy variable in Eq. (8). The primary assumption for IAST method is that enthalpies and surface area of adsorbed molecules is constant upon mixing, thus the surface covered by adsorbed mixture $\frac{A}{q_t}$ is

$$\frac{A}{q_t} = \frac{Ax_1}{q_1^0(P_1^0)} + \frac{Ax_2}{q_2^0(P_2^0)} + \dots + \frac{Ax_n}{q_n^0(P_n^0)}. \quad (11)$$

The total loading is calculated by:

$$q_t = q_1 + q_2 + \dots + q_n = \frac{1}{\frac{x_1}{q_1^0(P_1^0)} + \frac{x_2}{q_2^0(P_2^0)} + \dots + \frac{x_n}{q_n^0(P_n^0)}}, \quad (12)$$

where $q_1^0(P_1^0)$ is defined by unary, i.e. pure compound, isotherm fit, using $P_1^0, P_2^0 \dots$ from equation (10), (11). The loading q_i is determined by numerical calculation of set of equation (6), (7), ..., (11). (Krishna 2018.)

3.2.2 Activity coefficients and RAST

RAST method is derived from IAST for non-ideal adsorption. The nonideality in adsorbed phase is described by including activity coefficient (γ_i) to IAST. (Krishna 2018.)

The partial fugacity

$$f_i = P_i^0 x_i \gamma_i. \quad (13)$$

The Wilson model for activity coefficient

$$\ln(\gamma_i) = [1 - \ln(\sum_{j=1}^n x_j \Lambda_{ij}) - \sum_{k=1}^n \frac{x_k \Lambda_{ki}}{x_j \Lambda_{kj}}] (1 - \exp(-C \frac{\pi A}{RT})), \quad i=1, 2, \dots, n \quad (14)$$

where C is Constant (kg. mol^{-1}), and

Λ is the Wilson parameter, dimensionless.

3.3 Selectivity equilibrium

The selectivity predicts the separation of pair of components, component i and component j . At given constant temperature and independent of mixture composition. The selectivity S is (Krishna 2018)

$$S = \frac{q_i/q_j}{f_i/f_j}. \quad (15)$$

Where S is selectivity

q is loading, mol/ kg of framework

f is partial fugacity, Pa

i, j : component i and j

4 HYDROGEN BONDING AND MOLECULAR CLUSTERING

Because both water and ethanol are polar components, they compete for the same adsorption sites in the zeolite pores. The hydrogen bonding between molecular pairs forms clusters between the adsorbed guest molecules. The guest molecule pair may be water-water, water-ethanol, ethanol-ethanol. The strongest clustering is between water-ethanol pairs. The molecular clustering can be investigated by measurement of radial distribution function (RDFs) for distances between all combinations of O and H atoms of molecular pairs. However, it can be also illustrated by examining the unary isotherm and calculating the inverse thermodynamic factor. (Krishna 2018.)

$$\frac{1}{r_i} = \frac{\partial \ln q_i}{\partial \ln f_i} = \frac{f_i}{q_i} \frac{\partial q_i}{\partial f_i} \quad (16)$$

∂ : partial derivative

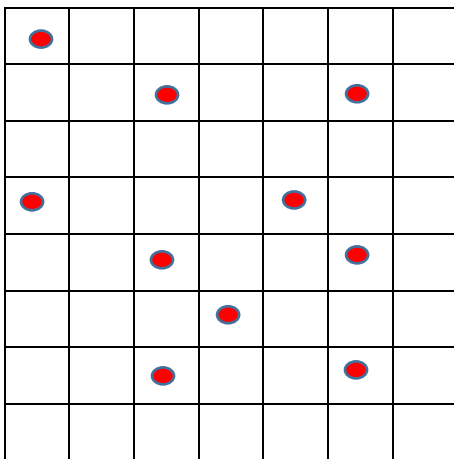
The fractional occupancy (θ_i) is calculated by

$$\theta_i = \frac{q_i}{q_{i,sat}}. \quad (17)$$

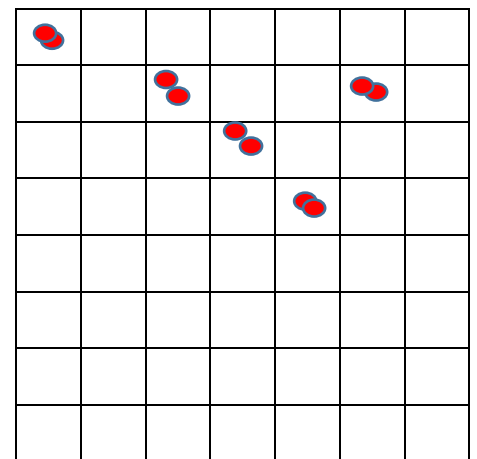
The inverse thermodynamic factor is calculated by

$$\frac{1}{r} = 1 - \theta_i. \quad (18)$$

The fractional occupancy of a compound can be evaluated using a pure component adsorption isotherm. In Eq. (16), the single site Langmuir equation has been applied. Figure 3 shows an example of molecule distribution in two cases: clustering and no clustering, imagining that there are 10 particles distributed in a square net containing 64 cells. If each particle occupies 1 cell, the number of vacant cells is 54 cells. Fractional occupancy θ_i is $10/64$; and the fractional vacancy θ_v is equal to $1 - \theta_i$, $\frac{1}{r} \leq 1$. If two molecules occupy same cell, the number of vacant cells is 59 cells. Even if there is no clustering molecule, this net can accept 59 molecules, the total molecule is 69, fractional vacancy θ_v is $69/64$ and the fractional vacancy θ_v is equal to $1 - \theta_i$, $\frac{1}{r} > 1$



a)



b)

FIGURE 3. a) Molecule distribution, no clustering, b) Molecule distribution, clustering (Krishna 2018)

5 MATERIALS AND METHODS

This thesis aimed to evaluate the adsorption behavior of ethanol- water mixture on different type of zeolite, which are CHA, DDR, MFI and FAU. Instead of evaluating by experiment, it was conducted by application of MATLAB programing. It simulated the adsorption phenomenon at given temperature (300K) with different fugacity. IAST and RAST methodologies were applied to simulate the adsorption isotherms.

5.1 Materials

In this study these zeolites were investigated: CHA, DDR, MFI, and FAU. Their adsorption parameters for the adsorption model was adopted from the supplementary material of the article: “Highlighting the origins and consequences of thermodynamic non-idealities in mixture separation using Zeolite and metal- organic frameworks” written by Krishna (2018). The shapes of the zeolite pores vary. The average pore diameter of these materials can be determined by Delaunay triangulation method. The pore diameters are shown in Table 4.

TABLE 4. Zeolite pore diameter and type (Krishna 2018).

Zeolites	Delaunay diameter (Å)	Type
DDR	3.65	Hydrophobic
MFI	5.16	Hydrophobic
FAU	7.37	Hydrophilic
CHA	3.77	Hydrophobic

The water molecule size is 2.8 Å, and for ethanol it is 4.5 Å. The topology of MFI is such that there are three-dimensional intersecting channels. On the other hand, CHA and DDR topology consist of cages separated by narrow 8-ring windows. FAU is type of zeolite has cages separated by large 8-ring windows. The pure component adsorption parameters for the investigated adsorbents are shown in Tables 5-8. Table 5 shows Dual-site Langmuir-Freundlich parameters for adsorption of water and ethanol at 300 K in all-silica FAU zeolite, including saturated loading q , v constant of site A and site B. These values are applied for calculation in IAST and RAST methodologies.

TABLE 5. Dual-site Langmuir-Freundlich parameters for adsorption of water and ethanol at 300 K in all-silica FAU zeolite (Krishna 2018).

Adsorbate	Site A			Site B		
	$q_{A, \text{sat}}$ (kg mol^{-1})	b_A (Pa^{-v_A})	v_a (-)	$q_{B, \text{sat}}$ (kg mol^{-1})	b_B (Pa^{-v_B})	v_B (-)
Water	16	1.54×10^{-121}	33	4.6	624×10^{-5}	1
Ethanol	2.5	3.19×10^{-13}	4.9	2.9	1×10^{-3}	1.05

Table 6 show Dual-site Langmuir-Freundlich parameters for adsorption of water and ethanol at 300 K in all-silica DDR zeolite, including saturated loading q , v constant of site A and site B. In site A the saturated loading of water is significantly higher than ethanol. In site B, it is slightly higher. b_A constant of water is much smaller than ethanol. v constant of water in site A is larger than ethanol. In site B, v constant of water and ethanol is equal. These values are applied for calculation in IAST and RAST methodologies.

TABLE 6. Dual-site Langmuir-Freundlich parameters for pure component water and ethanol at 300 K in all-silica DDR zeolite (Krishna 2018).

Adsorbate	Site A			Site B		
	$q_{A, \text{sat}}$ (kg mol^{-1})	b_A (Pa^{-v_A})	v_a (-)	$q_{B, \text{sat}}$ (kg mol^{-1})	b_B (Pa^{-v_B})	v_B (-)
Water	6.727	3.85×10^{-16}	4	2.219	1.73×10^{-5}	1
Ethanol	1.512	7.66×10^{-3}	1	0.645	8.59×10^{-6}	1

Table 7 shows Dual-site Langmuir-Freundlich parameters for adsorption of water and ethanol at 300 K in all-silica MFI zeolite, including saturated loading q , v constant of site A and site B. In both site A and site B, q_A of water is higher than its in ethanol. b_A constant of water is much smaller than ethanol. v constant of water in site A is larger than ethanol. In site B, v constant of water is higher than ethanol. These values are applied for calculation in IAST and RAST methodologies.

TABLE 7. Dual-site Langmuir-Freundlich parameters for adsorption of water, methanol, and ethanol at 300 K in all-silica MFI zeolite (Krishna 2018).

Adsorbate	Site A			Site B		
	$q_{A, \text{sat}}$ (kg mol^{-1})	b_A (Pa^{-v_A})	v_a (-)	$q_{B, \text{sat}}$ (kg mol^{-1})	b_B (Pa^{-v_B})	v_B (-)
Water	6.7	6.37×10^{-24}	6.2	3.6	1.09×10^{-5}	1.04
Ethanol	1.1	2.82×10^{-4}	2.7	1.7	1.91×10^{-2}	0.9

Table 8 shows Dual-site Langmuir-Freundlich parameters for adsorption of water and ethanol at 300 K in all-silica FAU zeolite, including saturated loading q , v constant of site A and site B. The saturated loading of water is higher than ethanol in both sides. b_A constant of water is much smaller than ethanol. v constant of water in site A is larger than ethanol. In site B, v constant of water is slightly higher than ethanol. These values are applied for calculation in IAST and RAST methodologies.

TABLE 8. Dual-site Langmuir-Freundlich parameters for pure component water, and 1-alcohols in CHA at 300K (Krishna 2018).

4Adsorb- ate	Site A			Site B		
	$q_{A, \text{sat}}$ (kg mol^{-1})	b_A (Pa^{-v_A})	v_a (-)	$q_{B, \text{sat}}$ (kg mol^{-1})	b_B (Pa^{-v_B})	v_B (-)
Water	16.64	7.86×10^{-59}	17	12.48	8.32×10^{-6}	1
Ethanol	2.77	7.93×10^{-5}	0.87	2.77	3.6×10^{-3}	1.14

The nonideality of the water and ethanol molecules in the respective zeolites is described with the activity coefficients between the adsorbates. These were found for FAU, DDR and MFI, while for CHA the parameters were not available. (Krishna 2018.) The parameters are shown in Table 9.

TABLE 9. Wilson non-ideality parameters for binary water/ethanol mixture adsorption (Krishna 2018).

	Λ_{12}	Λ_{21}	C (kg mol^{-1})
FAU	1.88	1.25	0.24
DDR	2.7	7.1	0.4
MFI	0.23	0.62	0.6

5.2 Method

The IAST and RAST adsorption models used in this study were available from DSc (Tech.) Jani Kangas from University of Oulu. The models had been implemented in MATLAB. The calculation was run on three main files: RAST_alkutiedosto.m (Script), RAST_pieni_polar_liquid_ethanol.m (function), RAST_Krishna_pieni_polar_liquid_ethanol (function). All the necessary calculation steps of IAST and RAST were formed in those two functions file. This task mainly worked on Script file.

5.2.1 Modelling water ethanol mixture loading on a zeolite as a function of partial fugacity

In the RAST_alkutiedosto.m file, these input were added: $q_{A, \text{sat}}$, $q_{B, \text{sat}}$, v_A , v_B , b_A , b_B , C , Λ_{12} , Λ_{21} . 'For' loop was applied to repeat the calculation 1000 times ($i=1:1000$). RASTI is the value defining if the program calculating uses IAST or RAST, if $\text{RASTI} = 1$, the adsorption equilibrium is calculated using the RAST, otherwise IAST is used in the mixture adsorption description. This simulation stops when the limit nearly zero. The calculated variables are saved. Then two variables are loaded, fugacity and loading, for plotting graph. The graph is plotted as logarithmic scale. Each type of membrane is calculated in separated file fitting these input value.

5.2.2 Modelling water ethanol mixture loading on a zeolite as a function of total fugacity

The procedure is same as modelling loading mass as function of partial fugacity. The only change is the plotting command, 'sum' function is used for combining two components partial fugacity into total fugacity.

5.2.3 Comparison of ethanol loading in different membranes

Ethanol loading is plotted as function of total fugacity. 'Hold on' syntax is used, so new plot is added on the previous plot. Thus, the ethanol loading of every membrane is illustrated on the same graph. An example of command for plotting ethanol loading on MFI membrane:

```
% Plot selectivity as function of total fugacity
%MFI
```

```
load RASTMFI005.mat fugTOTkoko qkoko;  
l=qkoko(2,:);  
loglog(sum(fugTOTkoko(:,:)),l,'k-');  
hold on;
```

The ethanol loading on the others membrane is plotted using the same command, only change the suitable save file at load command. The green sentence is comment, explaining what is calculated, and the remaining part is command for calculating.

6 RESULTS

This part shows the result of loading mass as function of partial fugacity and total fugacity of different zeolites. Moreover, the amount of ethanol loading at different total fugacity is performed, and the selectivity as function of total fugacity is provided as the aid of evaluating the efficiency of zeolites in adsorption. From these isotherms, the optimal point of operation of the adsorption process according to each zeolite were also figured out.

6.1 Loading mass as function of partial fugacity

In this part, the loading mass of water or ethanol is illustrated as function of partial fugacity of water or ethanol. The partial fugacity of each component is equal ($f_1 = f_2$). The temperature of adsorption is 300 K. The mass composition of adsorbing mixture is 50% EtOH.

6.1.1 FAU

The Fig. 4 shows the loading of ethanol and water as function of partial fugacity in FAU membrane. As can be seen in Fig. 4, the FAU zeolite prefers to adsorb a water molecule rather than an ethanol molecule, thus FAU is essentially hydrophilic material as stated also in Table 4. Results of the RAST and IAST models are not much deviated. The interesting point in FAU membrane is the adsorption behavior starting from the fugacity of $10^{3.3}$ Pa. The loading of water increases proportionally with fugacity. In IAST, limit loading of water component is about $10^{0.3}$ mol kg^{-1} and ethanol component is about 10 mol kg^{-1} at fugacity of $10^{2.1}$ Pa. RAST shows that the amount of adsorbed ethanol is higher than IAST. It is noteworthy that a point where the loading of water would be equal or higher than the one of ethanol does not exist when using FAU adsorbent.

In this zeolite adsorbent, both water and ethanol molecule can enter the pore, the because pore size is larger than molecule size. Thus, the kinetic selectivity controls the separation process. The bonding between water and adsorbent is stronger than between ethanol and adsorbent. More water molecules deposit on the surface of cages rather than ethanol molecules.

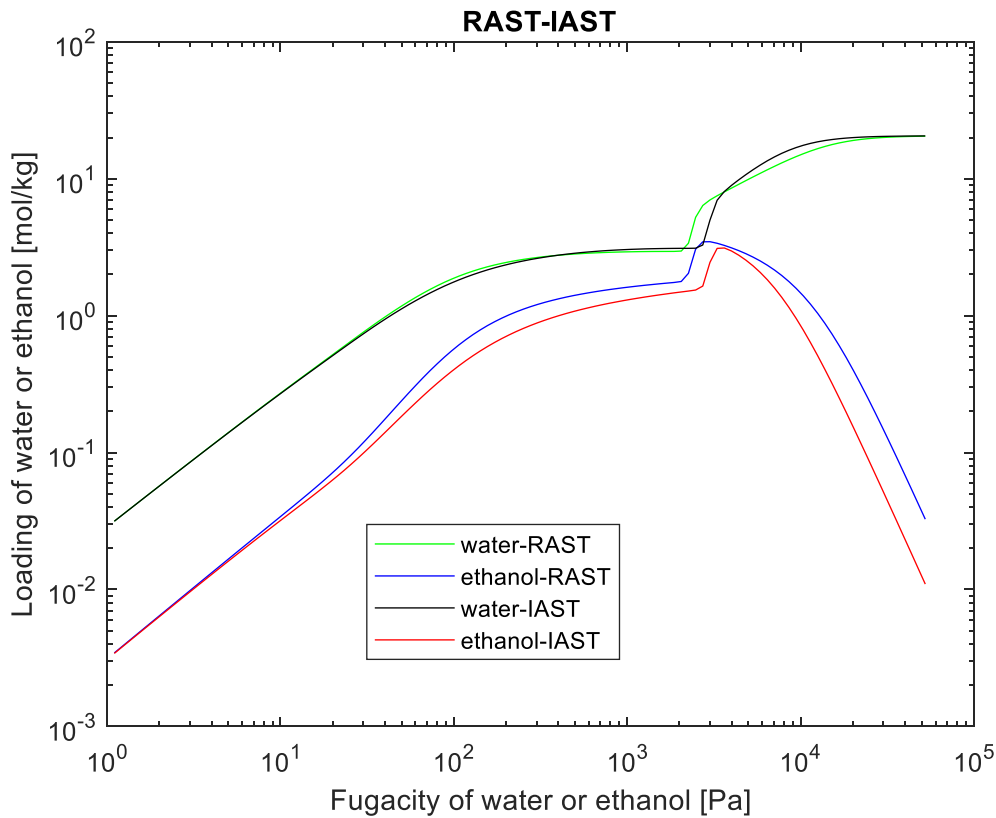


FIGURE 4. Adsorbed loadings of water and ethanol on a FAU zeolite as predicted by IAST and RAST. Temperature is 300 K. The fugacity of both ethanol and water in the feed mixture is the same.

6.1.2 MFI

The Fig. 5 shows the loading of ethanol and water as function of partial fugacity in MFI membrane. As can be seen in Fig. 5 MFI membrane is hydrophobic membrane because it adsorbs ethanol rather than water. Ethanol reaches limit loading at low fugacity, approximately 10 Pa. It is not much different between ethanol loading in IAST and RAST. The amount of water adsorbed in IAST is higher than in RAST. When the ethanol loading reaches its saturated value, the entropy of the system favors to adsorb more water molecules, causing loading of water to be equal to the loading of ethanol, it shown as crossing point in the graph. Both water and ethanol can deposit to the pores of the zeolite, because of their sizes are smaller than the pore size. However, graph 2 shows that the bonding between ethanol-adsorbent is stronger than water- adsorbent. The amount of ethanol deposits on cages is higher than water molecules. (Krishna 2015.)

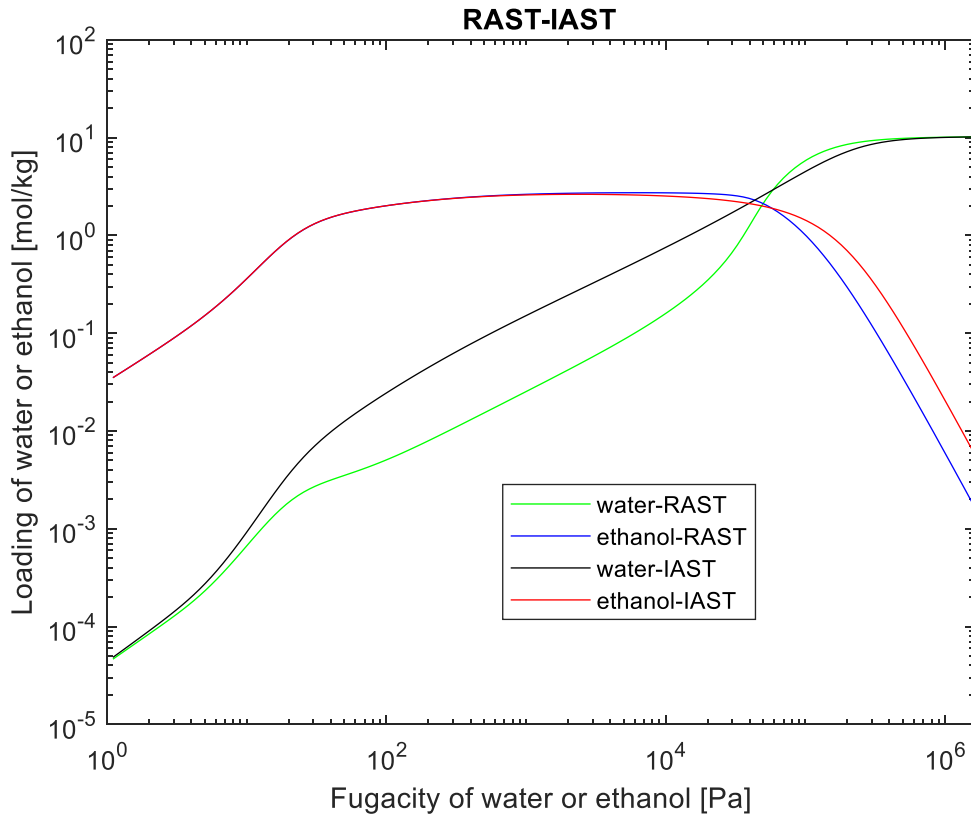


FIGURE 5. Adsorbed loadings of water and ethanol on MFI-zeolite at different fugacities with IAST and RAST. Temperature 300 K. The fugacity of both ethanol and water in the mixture is the same.

6.1.3 DDR

The Fig. 6 shows the loading of ethanol and water as function of partial fugacity in DDR membrane. Fig. 6 shows that this membrane adsorbs preferentially ethanol over water, so it is hydrophobic membrane. The noticeable point from RAST is that, in the presence of significant interactions between the adsorbents (non-idealities resembled by the activity coefficients), DDR zeolite adsorb more water molecule. It shows the strong attraction between water molecule and adsorbate. The ethanol adsorbate is not affected significantly by activity coefficient, yet water molecules. The amount of water loading calculated by RAST is largely deviated from IAST. The crossing point of water and ethanol is formed earlier in RAST than IAST.

The bonding between ethanol- adsorbent is stronger than water- adsorbent because the amount of adsorbed ethanol molecules is higher than amount of adsorbed water molecules. However, ethanol molecules size is larger than pore size ($3.8 > 3.65$), thus it may be stuck at the window instead of diffusing through the other sides. This hypothesis needs to be considered.

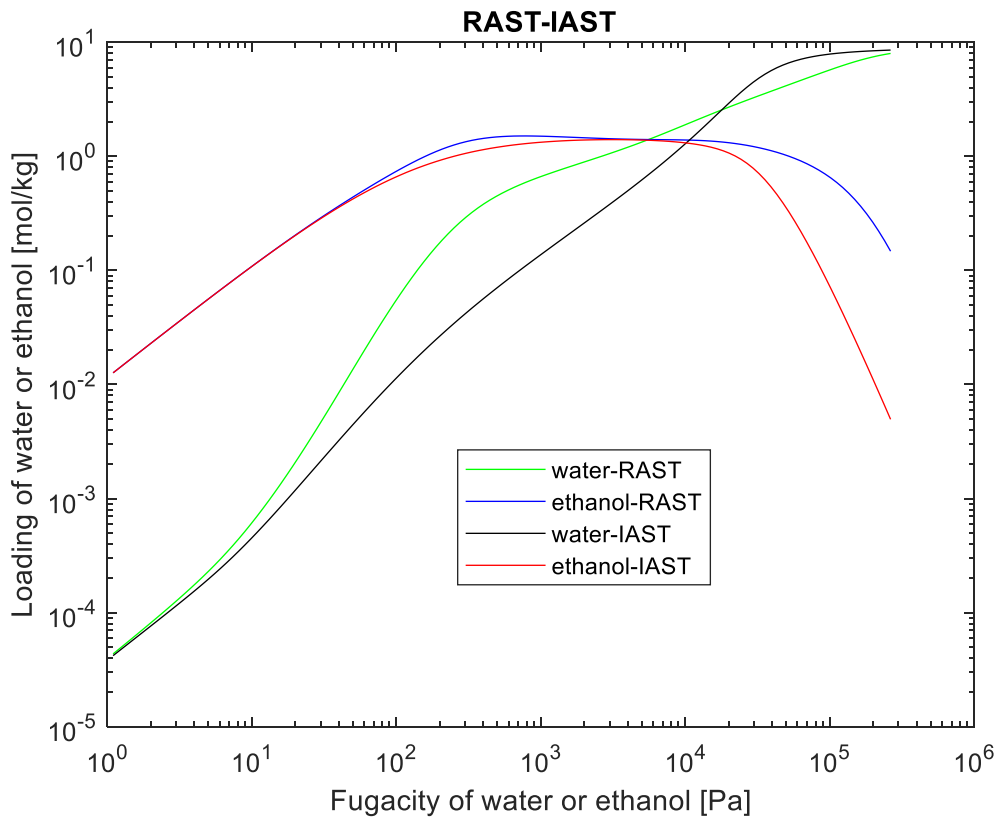


FIGURE 6. Adsorbed loadings of water and ethanol on DDR-zeolite at different fugacities with IAST and RAST. Temperature 300K. The fugacity of both ethanol and water in the mixture is the same.

6.1.4 CHA

The results from the model predictions with CHA zeolite are shown in Fig. 6. The behavior shows that the amount ethanol adsorbed is higher than the amount of water adsorbed, it confirms that CHA is a hydrophobic material. The following graph shows the adsorption of water and ethanol at ideal state. Because of shortage of Wilson parameter values for the mixture and CHA non-ideal interactions, RAST is not considered. This zeolite membrane adsorbed preferentially ethanol. The maximum loading of ethanol is nearly $10^{0.1}$ mol/kg at 10^2 Pa. If increasing fugacity, the entropy of system favors adsorbing water component, it is shown at crossing point in the graph, where loading of ethanol and water is equal. This

material is like DDR. The ethanol can be stuck at the window. The application of a DDR membrane for the separation of water- ethanol mixture needs more studies regarding the diffusion behavior.

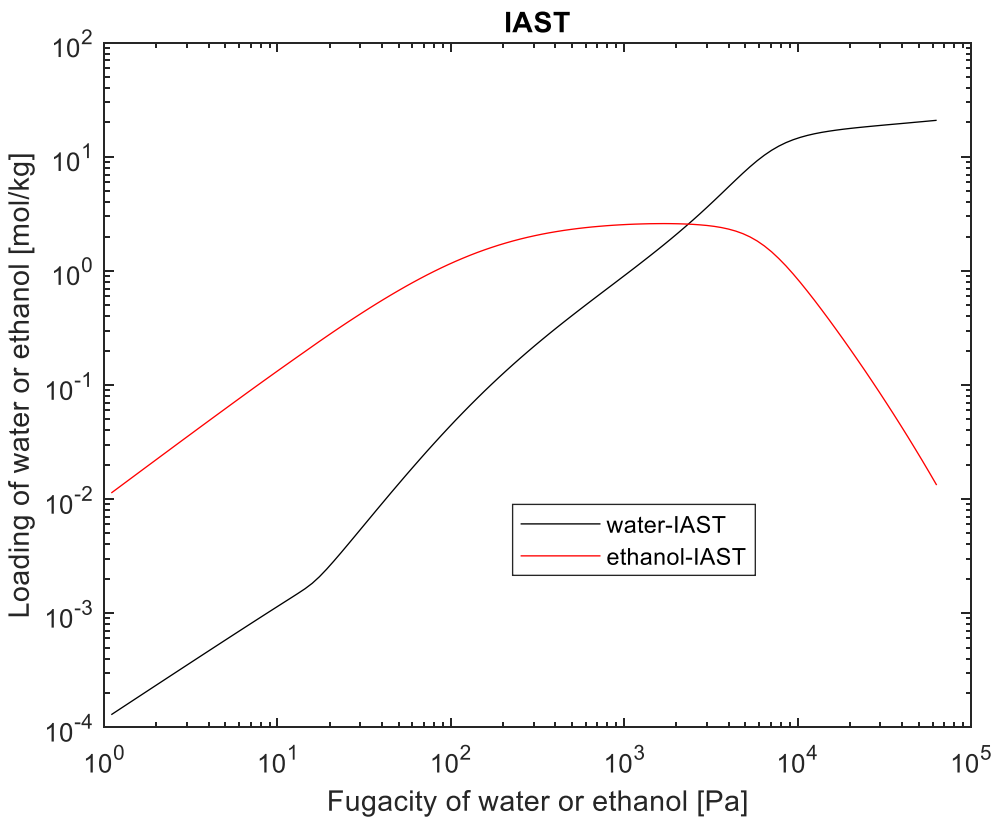


FIGURE 7. Adsorbed loadings of water and ethanol on CHA-zeolite at different fugacities with IAST. Temperature 300K. The fugacity of both ethanol and water in the mixture is the same.

6.2 Loading mass as function of total fugacity

This part shows the adsorption behaviors of different membranes if the mixture contains 5% EtOH. The concentration of ethanol production from common processes is only 5-10% by volume (ETIP). The traditional fermentation process is time consuming; it takes about 50-70 hours to produce final concentration of ethanol is 10-12% by volume (Bai et al. 2008) The mixture containing low concentration of ethanol cannot be separated by distillation alone, because a large amount of water needs to be vaporized. As a result, this process consumes high amount of energy. Membrane separation is considered as an alternative method to enhance the concentration and reducing energy consumption. Only RAST model is applied for examining the adsorption behaviors. It was implemented same as previous part, only changing in the mixture composition. The partial fugacity $f_1=f_2$ at 300 K.

6.2.1 MFI

In Fig. 8, the total loading of water or ethanol as function of total fugacity with MFI zeolite is shown. At low pressure, ethanol molecule is more adsorbed than water molecule. When ethanol reaches its saturated loading, the entropy of system favors adsorbing water molecule, thus loading of water and ethanol are same at $10^{3.7}$, the crossing point in the graph (Krishna 2018). Increasing fugacity causes ethanol adsorbate decreasing, and water adsorbate increasing until it reaches saturated point at $10^{4.1}$ Pa. The maximum loading of ethanol is $10^{0.9}$ mol/kg at about 10^6 Pa, and ethanol is 1 mol/kg at $f = 10^3$ Pa. The stepwise- liked shape of water isotherm show that there is formation of multilayer adsorption (Keller, J & Staudt, R 2005) (Seader et al. 2010)

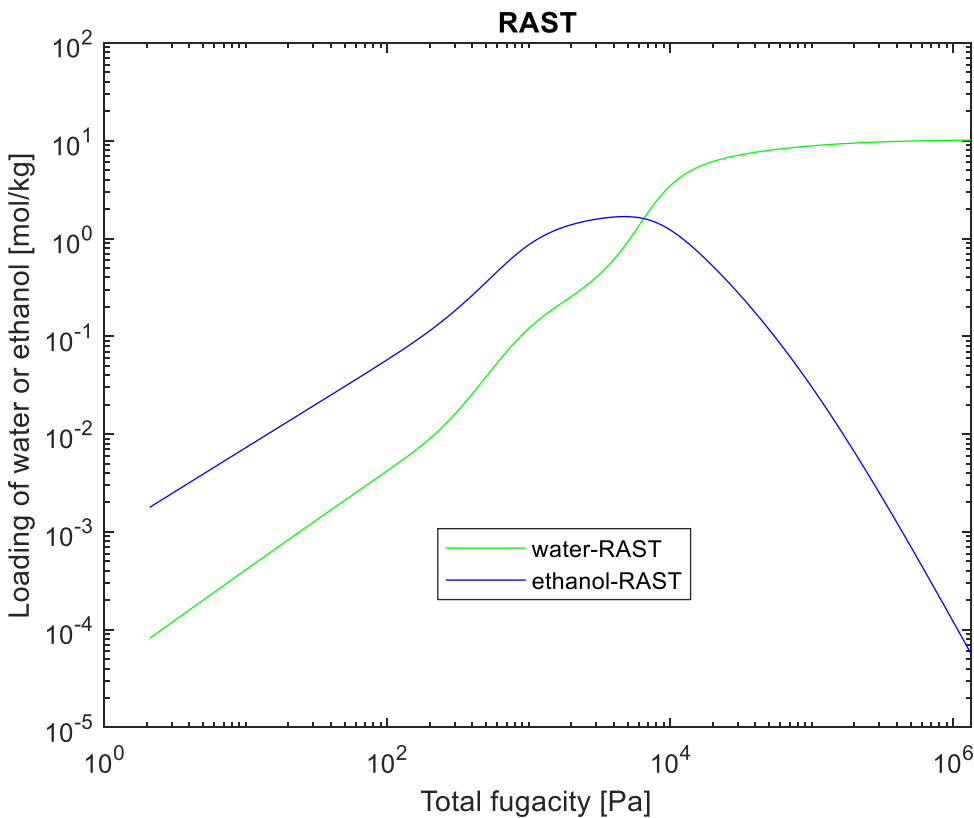


FIGURE 8. Adsorbed loadings of water and ethanol on MFI-zeolite at different total fugacities with RAST. Temperature 300K. The fugacity of both ethanol and water in the mixture is the same.

6.2.2 FAU

In figure 9, the total loading of water or ethanol as function of total fugacity with FAU zeolite is shown. The adsorption of water/ ethanol in FAU membrane is abnormal. The amount of loading of water is

significantly higher than ethanol. Even though when the water component reaches its saturate point, the entropy of system does not prefer to adsorb more ethanol. There is no point where loading of ethanol and water meet each other. The maximum loading of ethanol is about 10^{-1} mol/kg at $10^{2.2}$ Pa. The Fig. 9 confirms that FAU is suitable for dehydration of water/ ethanol mixture (Sato et al. 2008a, Zhu et al. 2009)

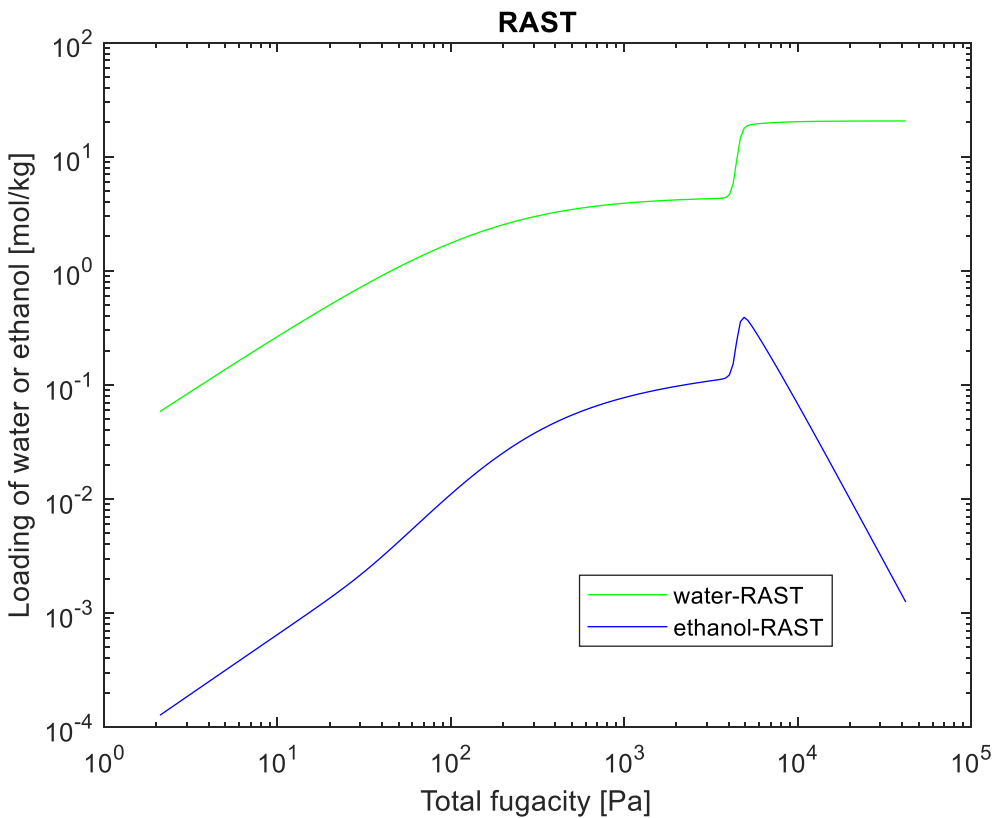


FIGURE 9. Adsorbed loadings of water and ethanol on FAU-zeolite at different total fugacities with RAST. Temperature 300K. The fugacity of both ethanol and water in the mixture is the same.

6.2.3 DDR

The adsorption in DDR zeolite dramatically fluctuates. It favors water adsorption at high pressure. Ethanol molecule is adsorbed easily formed monolayer at 10^6 Pa, saturated loading is 10^{-1} mol/kg. However, activity coefficient causes it raising to $10^{0.6}$ mol/kg at 10^7 Pa. After that, there are more layers formed.

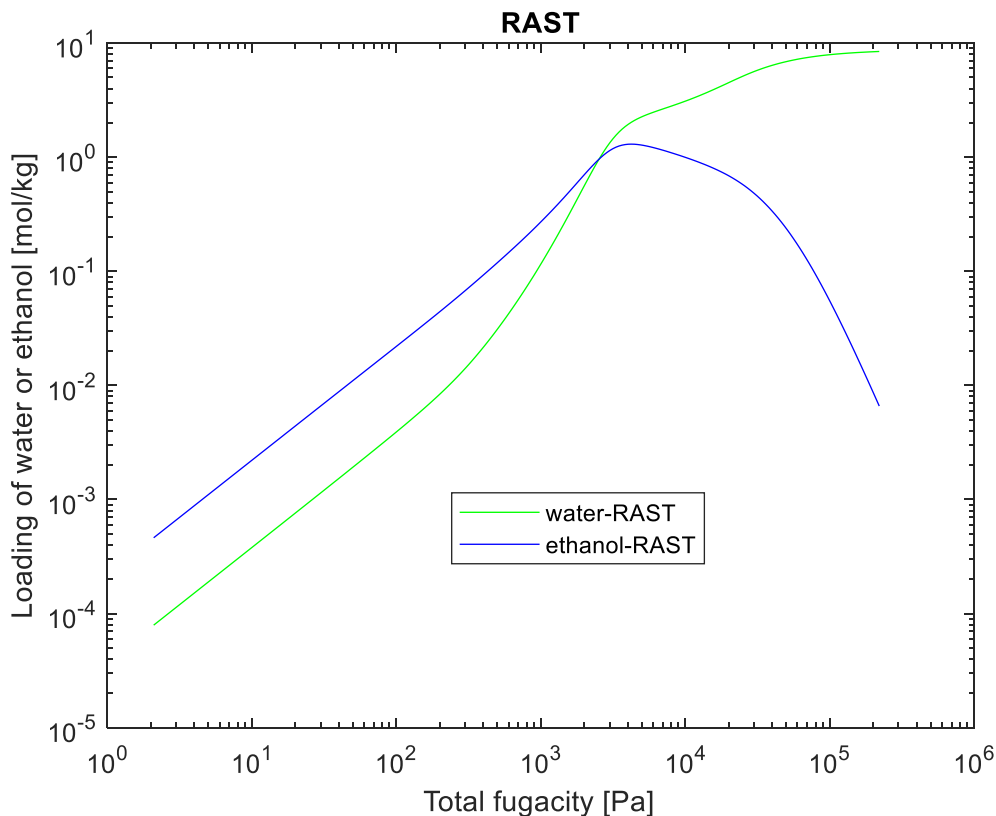


FIGURE 10. Adsorbed loadings of water and ethanol on DDR-zeolite at different total fugacities with RAST. Temperature 300K. The fugacity of both ethanol and water in the mixture is the same.

The ethanol adsorption is in this case monolayer adsorption. After saturation point, increasing fugacity causes ethanol loading to decrease. Water adsorbate performed in the opposite way, it forms multilayer adsorption, however it is not shown clearly on the graph, from 10^8 Pa the curve is benched at some point. The amount of adsorbed water and ethanol molecule is not significantly different compared to FAU.

6.2.4 CHA

Because the Wilson non-ideality parameters were not available for CHA for the binary water/ethanol mixture adsorption, adsorption on this zeolite is evaluated by IAST method only. This adsorbent is hydrophobic because it prefers to adsorb ethanol over water. The maximum loading of ethanol is about $10^{0.1}$ mol/kg at total fugacity is $10^{2.1}$ Pa. The loading of ethanol and water is equal at $10^{3.5}$ Pa.

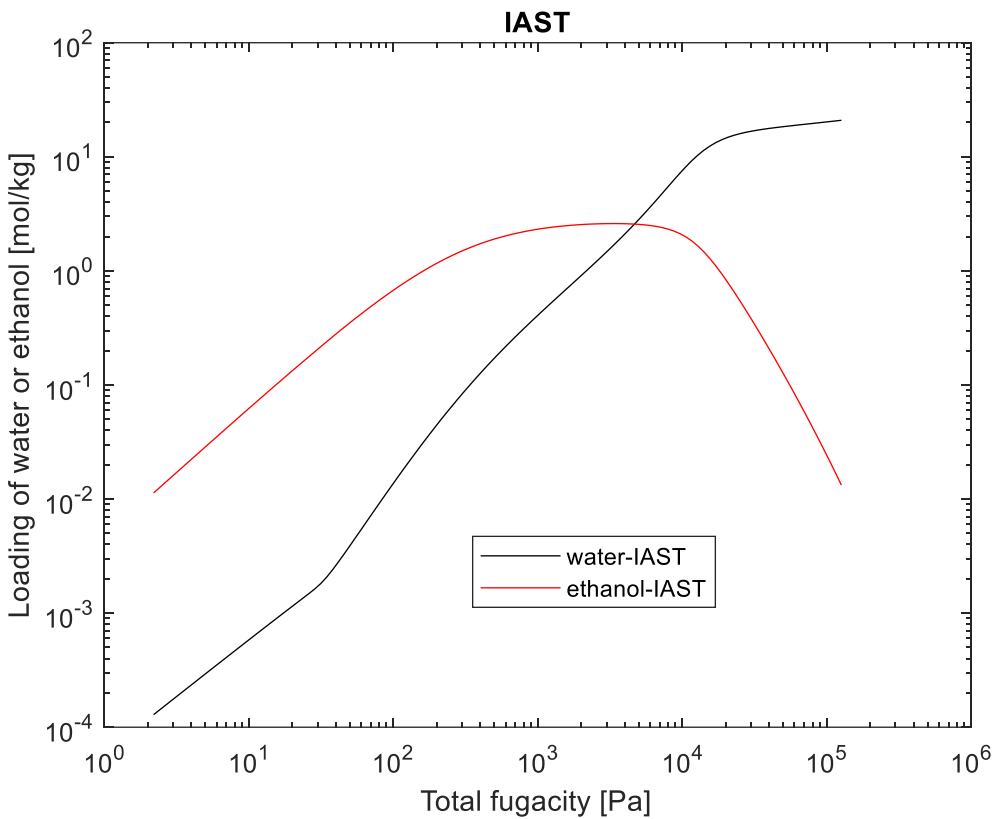


FIGURE 11. Adsorbed loadings of water and ethanol on CHA-zeolite at different total fugacities with IAST. Temperature 300K. The fugacity of both ethanol and water in the mixture is the same.

6.3 Comparison of ethanol loadings on different zeolites

Figure 11 shows the amount of adsorbed ethanol on four types of zeolites. CHA is the most efficient zeolite; however, the activity coefficient is not considered in this membrane compared to the others. Thus, this result requires further study. Among MFI, DDR, and FAU, the amount of ethanol adsorbed in MFI is highest, then DDR, and FAU is the last one. Ethanol loading reaches its saturation level in FAU the earliest, however also its the maximum loading of ethanol is the lowest. When increasing fugacity until $10^{4.4}$ Pa, the order of ethanol loading is changed. The amount of ethanol loading in CHA zeolite and MFI zeolite is less than it is in DDR and loading of ethanol in FAU is still least.

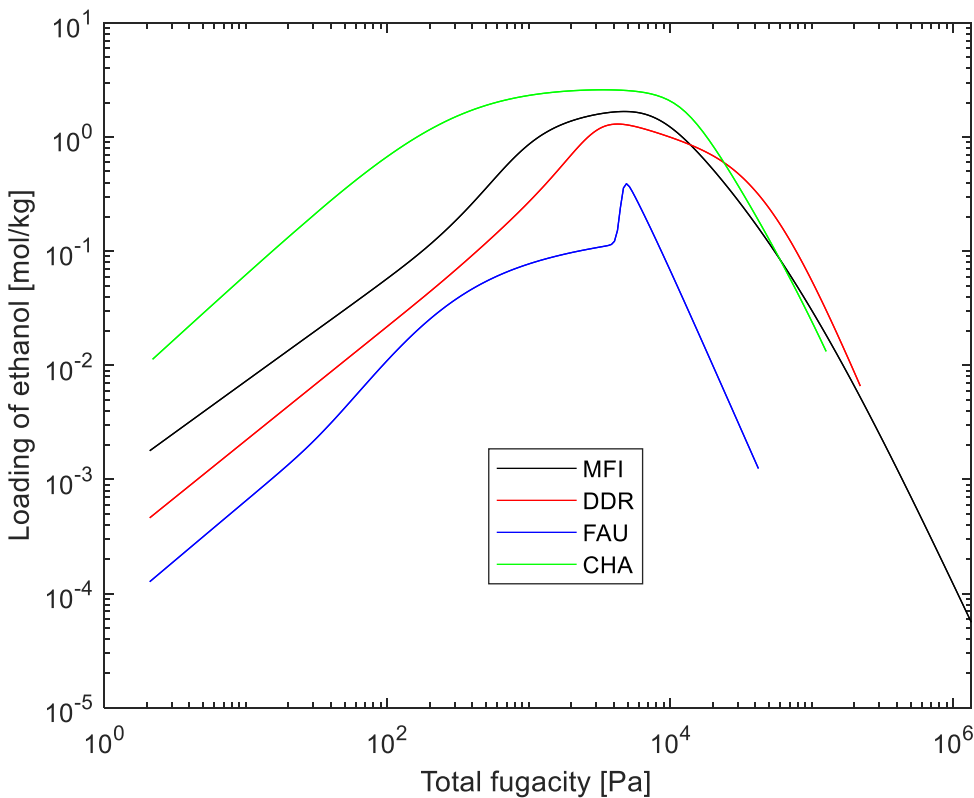


FIGURE 12. Ethanol loading (mol/kg) on different type of membrane at 300K, $f_1=f_2$

6.4 Ethanol/Water adsorption selectivity

Figure 13 illustrates the selectivity of ethanol over water at different total fugacity. Fig. 13 shows the selectivity of ethanol/ water at 300K, $f_1=f_2$. The selectivity is calculated by Eq. (18). Increasing fugacity causes the decrease of the ethanol selectivity. CHA owns highest selectivity at low fugacity; however, these values were calculated with IAST, i.e. the effect of the non-idealities have not been taken into account. Considering MFI, DDR, FAU, the selectivity of MFI is highest, then DDR and FAU is lowest. Increasing fugacity causes changing in ethanol/ water selectivity. In the range of total fugacity 1000 Pa-12590 Pa, ethanol selectivity in MFI zeolite ranks first, then CHA zeolite, and followed by DDR, the order of ethanol/ water selectivity is still in final position. After 12590 Pa, the order is changed again, DDR zeolite possesses highest selectivity, then MFI switches from first position into second one, followed by CHA, and FAU remains its final position.

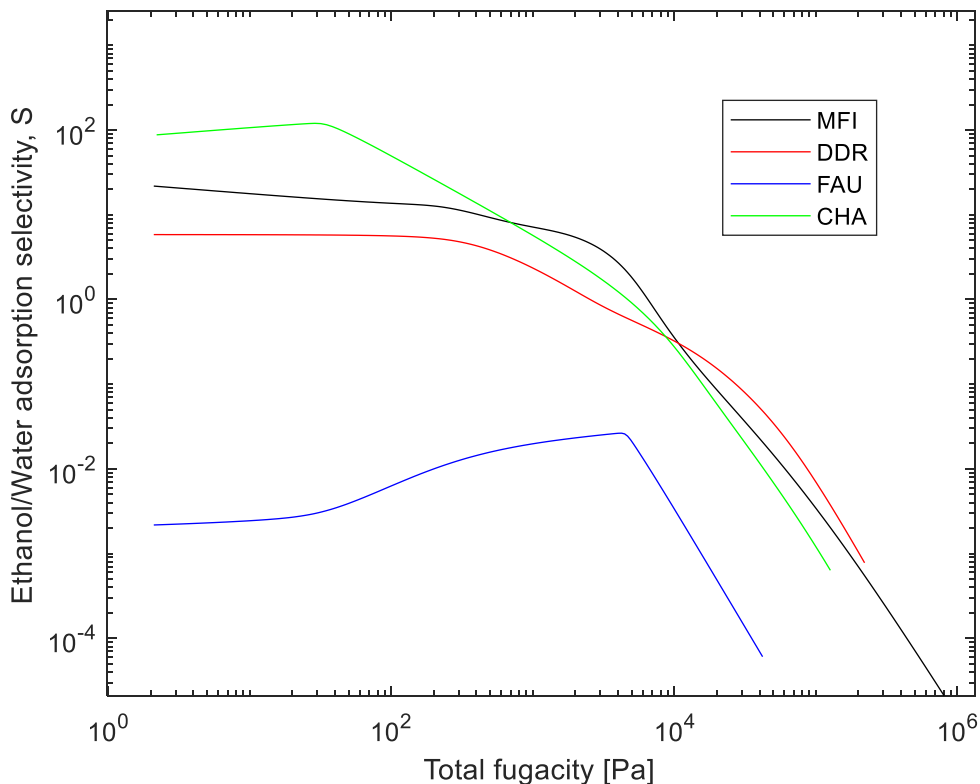


FIGURE 13. Selectivity on different type of membrane, Ethanol/Water

When FAU zeolite is applied, the amount of ethanol deposited on pore cage is much lower than the one of water. Thus, a large amount of water is removed from the mixture, the concentration of ethanol increasing. It shows highest ethanol concentration is at about 100 Pa. However, at this point the loading

of water is low (see Fig 6), so it is not optimal and economic alternative. The optimal point is at 316 Pa, and the concentration of adsorbed mixture at this point containing on 1.5% ethanol. The selectivity of MFI and amount of ethanol loading of MFI is higher than DDR. Furthermore, if ethanol is stuck at DDR zeolite window, causing diffusing difficulty through pore (see 4.1.3). Thus, MFI membrane is more efficient than DDR in the separation of a water-ethanol mixture.

7 DISCUSSION

The adsorption behavior of the zeolites illustrated are different when using either IAST or RAST. When predicting the adsorption behaviors on zeolite membrane, the activity coefficient must be added. When predicting the adsorption on CHA, MFI, DDR, FAU, the activity coefficient affects water adsorbate significantly compared to the ethanol adsorbate. The asymptotic point of water and ethanol is different accordingly to type of zeolite. Increasing fugacity, the entropy of system adsorbs preferentially water molecules, causing the loading of water is equal to ethanol, which is show at crossing point in these figures. However, in FAU zeolite, crossing point does not exist. The step-like isotherm of FAU membrane is an interesting point that need to be explained. It may be because of its dehydration characteristic. The amount of ethanol entering the pore is in minor quantities.

Among these four membranes, only FAU is hydrophilic membrane. FAU membrane is basically a good material for dehydration of water/ethanol mixture. Among the hydrophobic zeolite membrane, CHA is the most efficient one; however, the activity coefficient is not introduced in the calculations. Thus, the results have uncertainties. When comparing the selectivity of ethanol/water, MFI adsorbs more ethanol molecules than DDR.

Considering the zeolite pore size and adsorbate size, DDR membrane and CHA membrane yields an issue is the pore size is smaller than both water and ethanol molecule size. Thus, the molecule can be stuck at the pore window instead of diffusing through. Thus, there is not separation process occurred. It requires further study for adequate conclusion. If these hypotheses are true, MFI is the best zeolite for adsorbing ethanol, FAU is the most efficient zeolite for dehydration water/ ethanol mixture.

8 CONCLUSION

When operating an adsorption process, the total fugacity should be about 100 Pa. At lower fugacity, ethanol concentration is higher, however the amount of loading is low, it is not optimal process. The purified ethanol produced by pervaporation also needs another separation method such distillation to increase the concentration of ethanol. Increasing total fugacity, the entropy of system adsorbs preferentially water components, yet FAU zeolite is exceptional.

Through this thesis, the adsorption isotherm confirms that both water and ethanol component can enter the pores. However, the adsorbed amounts vary depending on the type of the zeolite. The adsorption isotherm also helps to identify whether the zeolite is hydrophobic or hydrophilic. Because the adsorption isotherm shows the amount of loading of components, at same fugacity and constant temperature, if the loading of organic compound is higher than loading of water component, it is hydrophobic. In the case, the loading of water is higher than loading of organic compound, as a result it is hydrophilic.

The shape of isotherm in these zeolites are different to each other. The clustering of molecules because of hydrogen bonding affects the distribution of adsorbate molecules on the zeolite surface. It is shown by the inverse of thermodynamic as function of total fugacity. However, there is no evidence to prove it in this thesis, thus it is one limitation of this thesis.

The modeling to predict the adsorption behaviors has been widely applied and compared to other experimental method which is an acceptable method. However, this modelling result is not compared to any experimental result; thus, the reliability is limited. The deviations between modelling and experimental result is not compared. Understanding of the location of molecules on the surface of membrane help explain more detail about the effect of thermodynamic in adsorption.

This thesis investigated the adsorption behaviors of low concentration ethanol mixtures, 5% by weight. The amount of loading on zeolite is quite low, the maximum is about $10^{0.1}$ mole /kg of framework, in CHA zeolites, its lower in MFI, DDR and FAU zeolite. The saturated point is different in these membranes.

IAST is not applicable for calculation of adsorption isotherm for water/ ethanol mixture. The results provided by IAST and RAST are not the same, thus the effect of the activity coefficients must be considered. Because activity coefficients also affect the adsorption behaviors, RAST method is more feasible than IAST. The amount of loading is dependent strongly on the fugacity. Comprehensive understanding about separation process of ethanol/ water requires fulfillment of analysis about both adsorption, diffusion, and diffusivity. When designing separation process, RAST method utilization is essential.

In general, the application of zeolite membrane is a promising for dehydration of water ethanol mixture. It can reduce cost, energy consumption, and ecofriendly. It enhances the concentration of ethanol produced in industry. In the future, when using a zeolite membrane for water/ethanol separation, also the durability of membrane should be considered.

REFERENCES

- Anderson, W, A. & Bai, F, W. & Moo- Young, M. 2008. Ethanol fermentation technologies from sugar and starch feedstocks. Elsevier.
- Bourg, C. & Reime, M . & Smit, B. & Oldenburg, M. 2014. Introduction to carbon capture and sequestration. Imperial college press.
- ETIP Bioenergy. Available at: <http://www.etipbioenergy.eu/value-chains/conversion-technologies/conventional-technologies/ethanol-fermentation>. Accessed: 9 May 2020.
- Evaporation. Britannica. Available at: <https://www.britannica.com/science/evaporation> . Accessed: 28 April 2020.
- Fechtner, M. & Kiel, A. 2018. Efficient simulation and equilibrium theory for adsorption processes with implicit adsorption isotherms – Ideal adsorbed solution theory. Elsevier.
- Fornstedt, T. & Forssen, P. & Samjelsson, J. 2013. Chapter18: Modelling of preparative liquid chromatography. Liquid chromatography: Fundamentals and instrumentation. Elsevier.
- Jani, K. Separation process modelling. 2014. Finland: Oulu university.
- Jasper,M,van, Baten. & Krishna, R. & Richard, B. 2018. Highlighting origins and consequences of thermodynamic non- idealities in mixture separation using zeolite and metal organic frameworks. Elsevier.
- Jasper,M,van, Baten. & Krishna, R. & Richard, B. 2018. Supplementary material. Highlighting origins and consequences of thermodynamic non- idealities in mixture separation using zeolite and metal organic frameworks.
- Krishna, R. Physical Chemistry. Chemical Physic., 17 (2015), pp. 39-59.
- Kuppler,J. & Li,J,R. & Zhou, H,C. Selective gas adsorption and separation in metal–organic frameworks. 2009.
- Leppäjärvi, T. 2015. Pervaporation of alcohol/water mixture using ultrathin zeolite membranes. Finland: University of Oulu.
- Li, Y. & Liu, J. & Zhou, H. & Yang, W. & Zhu, G.2009. Microwave synthesis of high performance FAU-type zeolite membranes: Optimization, characterization and pervaporation dehydration of alcohols.
- Malara, C. & Pierini, G . &Viola, A. 1992. Nuclear science and technology. Correlation, analysis and prediction of adsorption equilibria. Available at: http://publications.europa.eu/resource/cellar/e17a61a1-5005-44c7-a073-d7ced9995bfb.0001.02/DOC_1 . Accessed:13 April 2020.
- Mc Cabe, Warren L. & Smith, Julian C. & H, Peter. 2005. 7th edition. Unit operation of chemical engineering. Mc Grow Hill cop.

Mohanty, K. & Purkait, K. 2011. Membrane technologies and applications. p68. CRC press.

Nakane, T. & Sato, K. & Sugimoto, K. 2008. Mass-production of tubular NaY zeolite membranes for industrial purpose and their application to ethanol dehydration by vapor permeation.

Ruthven, M. 1984. Principle of adsorption and adsorption process. John Wiley and Sons. Canada.

Sing K.S.W. et al. Reporting Physisorption Data for Gas/Solid Systems with Special Reference to the Determination of Surface Area and Porosity, IUPAC Recommendations 1984, Pure & Appl. Chem., 57 (1985), 603-619.

Stewarr Slater, C. 1991. A Review of: "Pervaporation Membrane Separation Processes", Separation and Purification Methods.

Water molecule size. Available at: <https://bionumbers.hms.harvard.edu/bionumber.aspx?s=n&v=6&id=103723> Accessed: 28 April 2020.

Zuo, X. & Zhu, G. 2019. Microporous material for separation membranes. Germany: Wiley- VCH.

RAST_alkutiedosto script, it is the fundamental MATLAB script applied for calculation of adsorption isotherm in this thesis. It is built and permitted by DSc (Tech). Jani Kangas.

```

% RAST adsorption calculation initialization file
% Krishna et al. 2018 supplementary parameters
% MFI, 300 K
% Compounds Water(1) ethanol(2)
% Saturation loadings qsatA and qsatB
qsatA=[6.7 1.1];
qsatB=[3.6 1.7];
% Adsorption coefficients for A and B adsorption sites
bA=[6.37e-24 2.82e-4];
bB=[1.09e-5 1.91e-2];
% Exponents for the fugacities
vA=[6.2 2.7];
vB=[1.04 0.9];
% Freundlich pure component adsorption isotherm in use if FRAUND==1
FRAUND=1;
% RAST or IAST calculation?, If RAST calculation RASTI=1, IAST calculation
% RASTI=0
RASTI=1;
if RASTI==1
% RAST activity coefficients parameters
% MFI, 300K
    C=0.6;
    lambda12=0.23;
    lambda21=0.62;
else
    % IAST calculation
    C=0;
    lambda12=0;
    lambda21=0;
end

for i=1:1000
    % Composition of adsorbing mixture, y
    y=[0.5 0.5];
    if i==1
        % Starting fugacities for both [Pa]
        fugTOT=[1 1];
    else
        fugTOT=fugTOT*1e5;
    end
    % Parameters which control the increase of fugacity for one for-loop to
    % another
    muutos=0.05*sum(fugTOT);
    muutosEtOH=18/949*(sum(fugTOT)+muutos);
    muutosH2O=931/949*(sum(fugTOT)+muutos);
    fugTOT=[muutosH2O muutosEtOH]./1e5

    % Pressure scaling coefficient
    scalingupper=sum(fugTOT)*1000;
    % Which compounds are present in the mixture 1= water, 2=ethanol
    komponentti=[1 2];
    qsat=[];
    KA=[];

```

```

% Temperature [K]
T=300;
if i==1
    % Estimate for the adsorption model solution, X0alku
X0alku=[4.4914; 0.0100; 0.0004; 0.9996];
else
    % if we have for loop 2 or higher, we apply the previous solution as
    % the estimate for the next round
    X0alku=X;
end
% Tells us has the adsorption solution converged. If we have not solved yet
% the model, EXITFLAGalku=0
EXITFLAGalku=0;

[q,theta,y,T,EXITFLAG,X,xads]=RAST_pieni_polar_liquid_Ethanol(y,fugTOT,kompo-
nentti,qsat,KA,T,X0alku,EXITFLAGalku,qsatA,qsatB,vA,vB,bA,bB,FRAUND,scal-
ingupper,C,lambdal2,lambdal1)
% EXITFLAG>0, if the solution has converged, if EXITFLAG<1 then the
% solution has not converged
if EXITFLAG<1
    'The solution has not converged'
    break
end
% Storage of the solution to Xkoko and loadings to qkoko
Xkoko(:,i)=X;
qkoko(:,i)=q;
fugTOTkoko(:,i)=fugTOT.*1e5;
% Plots the fugacities versus loadings on a log-log diagram
% loglog(sum(fugTOT*1e5),q(1),'kx',sum(fugTOT*1e5),q(2),'rx')
% if RASTI==1
%     title('RAST');
% else
%     title('IAST');
% end
% legend('Water','Ethanol');
% xlabel('Fugacity of water or ethanol [Pa]');
% ylabel('Loading of water or ethanol [mol/kg]');
hold on;
save RASTMFI005.mat fugTOTkoko qkoko;
pause(0.5);
end
load RASTMFI005.mat;
loglog(sum(fugTOTkoko(:,:)),qkoko(1,:), 'g-', sum(fugTOTkoko(:,:)),qkoko(2,:), 'r-');
title('RAST');
xlabel('Total fugacity, [Pa]');
ylabel('Loading of ethanol, [mol/kg]');

```